

Optimization of a Novel Melt-Growth Heat Treatment of $\text{YbBa}_2\text{Cu}_3\text{O}_{7-\delta}/\text{Ag}$ Tapes

Zili Zhang, Jianyi Jiang, Qiuliang Wang , David C. Larbalestier, and Eric E. Hellstrom

Abstract—A novel melt-growth heat treatment of $\text{YbBa}_2\text{Cu}_3\text{O}_{7-\delta}$ (Yb123) powder in Ag-sheathed tape has been established as a necessary first step to form aligned Yb123 grains in a powder-in-tube (PIT) conductor. The heat treatment parameters including the rate at which the atmosphere was changed from Ar to pure O_2 , the heat treatment temperature, and the time during which the melt transformed back to Yb123 were investigated to find the optimum parameters for reforming Yb123 in Ag-sheathed tape. The Yb123 purity after being reformed is insensitive to the rate at which the atmosphere was changed. The optimized parameters are 910 °C for 48 h to reform Yb123.

Index Terms— $\text{YbBa}_2\text{Cu}_3\text{O}_{7-\delta}$, superconductor, melt and growth, oxygen partial pressure.

I. INTRODUCTION

THE high temperature superconductor $\text{REBa}_2\text{Cu}_3\text{O}_{7-\delta}$ (RE123; RE = rare earth – also called REBCO) has significant advantages of high current density (J_c), high irreversibility field (H_{irr}), and high critical transition temperature (T_c) compared to other superconductors. There have been extensive fundamental studies and also technological studies for applications in areas such as transmission cables [1], [2], insert magnets for high-field magnets [3], [4], fault current limiters [5], [6], and generators for wind turbines [7]. The RE123 coated conductors require bi-axial texture to achieve high J_c [8], [9], and both the Ion Beam Assisted Deposition (IBAD) and Rolling Assisted

Biaxially Textured Substrate (RABiTS) methods to make the textured coated conductor are too complicated and expensive for many applications [10].

If it were possible to make a high- J_c RE123 tape or round wire using the simpler powder-in-tube (PIT) method, it would be great improvement for RE123 applications. However, multiple attempts to make a high J_c wire since Y123 was first discovered have yielded Ag-sheathed conductors whose highest critical current (I_c) was only 5.02 A at 77 K self-field [11], which is due to lack of texture in the Ag-sheathed conductor. In 2014, Larbalestier *et al.* reported a significant increase in J_c in Ag-sheathed $\text{Bi}_2\text{Sr}_2\text{CaCu}_3\text{O}_8$ (Bi-2212) round wire, in which highly aligned Bi-2212 grains formed naturally as Bi-2212 reformed from the melt on cooling [12]. Using Bi-2212 as a model, we selected $\text{YbBa}_2\text{Cu}_3\text{O}_{7-\delta}$ (Yb123), which has the lowest melting temperature of the RE123s [13] to attempt to melt and regrow Yb123 in Ag-sheathed tape.

In this paper, we investigated details of the heat treatment that varies the $p\text{O}_2$ and temperature during the heat treatment to grow Yb123 from the melt in a Ag-sheath. The parameters we studied included the rate at which the atmosphere was changed, and the heat treatment temperature and time during which Yb123 grew from the melt. We also investigated the effect that the purity of the as-synthesized Yb123 has on the amount of Yb123 that grew from the melt.

II. EXPERIMENTAL PROCEDURES

Powder Preparation: Yb123 powder was synthesized by a solid-state reaction. Yb_2O_3 (99.99% Alfa Aesar), BaCO_3 (99.8% Baker Analyzed) and CuO powder (99.995% Alfa Aesar) were mixed in the stoichiometric ratio to form Yb123, ground together, pressed into a pellet, and heat treated in a tube furnace at 920 °C for 24 h under flowing O_2 . The pellet was ground, repressed and reheated until the powder was essentially pure Yb123 by x-ray analysis. We judged the purity by the ratio of the intensity of the strongest x-ray peaks of Yb123 to Yb211 ($\text{Yb}_2\text{BaCuO}_x$), i.e., Yb123:Yb211. This ratio was typically 4, which we refer to as standard purity Yb123. Unless specifically mentioned otherwise, the experiments described below had a ratio of 4. For one set of experiments we did several additional grind, press, sinter sequences that raised this ratio to 8, which we refer to as high purity Yb123.

Tape Preparation: The Yb123/Ag tape was fabricated by the Powder-In-Tube (PIT) method. Pure, as-synthesized Yb123 powder was packed into Ag tubes (OD: 6.35 mm; ID: 4.35 mm).

Manuscript received September 18, 2017; accepted January 16, 2018. Date of publication January 23, 2018; date of current version March 13, 2018. This work at the national high magnetic field laboratory was supported in part by the National Science Foundation Cooperative Agreement no. DMR-1157490, and in part by the State of Florida. The work of Z. Zhang was supported in part by the National High Magnetic Field Laboratory's Schuler Postdoctoral Fellowship, and in part by the National Natural Science Foundation of China under Grant 51702316. The work of Q. Wang was supported in part by the National Natural Science Foundation of China under Grants 51307163, 11745005, and 51477167, and in part by the Key Research Program of Frontier Sciences, Chinese Academy of Sciences, under Grant QYZDJ-SSW-JSC012. (Corresponding author: Qiuliang Wang.)

Z. Zhang was with the Applied Superconductivity Center, National High Magnetic Field Laboratory, Tallahassee, FL 32310 USA. He is now with the Institute of Electrical Engineering, Chinese Academy of Sciences, Beijing 100190, China.

J. Jiang, D. C. Larbalestier, and E. E. Hellstrom are with the Applied Superconductivity Center, National High Magnetic Field Laboratory, Tallahassee, FL 32310 USA, and also with the Florida State University, Tallahassee, FL 32306 USA.

Q. Wang is with the Key Laboratory of Applied Superconductivity, Institute of Electrical Engineering, Chinese Academy of Sciences, Beijing 100190, China (e-mail: qiuliang@mail.iee.ac.cn).

Color versions of one or more of the figures in this paper are available online at <http://ieeexplore.ieee.org>.

Digital Object Identifier 10.1109/TASC.2018.2796385

The tube was drawn down to 4.62 mm diameter, and then it was rolled into a flat tape with a 10% reduction in thickness in each rolling pass to a final thickness of 1.02 mm.

Heat Treatment Processes: Sections of the Yb123/Ag tape (10 cm long) were heat treated in a tube furnace in which we could change the atmosphere from flowing Ar to flowing O₂. During the heat treatments, we changed the temperature and also changed the atmosphere in the furnace from Ar to O₂ by flowing O₂ to replace the Ar. The oxygen partial pressure (pO₂) in the furnace was measured with a zirconia oxygen sensor. The details of the specific heat treatment schedules and the results from each heat treatment are given in the Results and Discussion Section.

Sample Characterization: The phase analysis of the samples was characterized by Cu K α x-ray diffraction (XRD) using a Philips goniometer. For x-ray analysis, ceramic material was extracted from inside the tape samples after the heat treatment and ground into a powder. The regrown Yb123 was characterized by the Yb123:Yb211 intensity ratio.

III. RESULTS AND DISCUSSION

Fig. 1(a) shows our heat treatment schedule to melt and regrow Yb123 in Ag-sheathed tapes. There are four lines in Fig. 1(a): the red solid line at the top is the actual temperature schedule for the entire process; the purple dotted line shows the melt temperature of Yb123 due to the presence of Ag; the blue dashed line in the middle shows the change of the atmosphere in the furnace; and the green dash-dot line at the bottom schematically shows the expected phases present in the tape. The heat treatment consists of three steps. In step 1 the sample is heated in flowing Ar to 940 °C at 10 °C/min, held for 2 h to melt the Yb123, and then the temperature is decreased to 910 °C at around 10 °C/min. In step 2, the gas is changed from Ar to O₂ at various flow rates. In step 3, the sample is held for an additional 48 h at 910 °C in flowing O₂, and is finally cooled to room temperature in the furnace under flowing O₂. The heat treatment was designed to melt Yb123 in step 1, and the presence of the Ag decreased the melt temperature of Yb123 from 936 °C in pure O₂ to 905 °C in Ar [shown as by the purple dotted line in Fig. 1(a)]. In step 2, the melting temperature of Yb123 increased as O₂ replaced Ar in the furnace, which nucleated and grew Yb123 from the melt. In the step 3, the nucleation and growth of Yb123 finished and the sample was cooled to room temperature.

Fig. 1(b) shows the XRD patterns of fully heat-treated Yb123/Ag tape after the heat treatment process in Fig. 1(a). The two strongest peaks, which are around 32°, correspond to the (103) and (013) peaks of tetragonal Yb123. They show that Yb123 is the main phase after the heat treatment. However, there are also strong peaks from Yb211 and BaCuO₂ in the pattern. The Yb123:Yb211 intensity ratio from Fig. 1(b) is 1.91, which shows that although the heat treatment process can reform Yb123 from the melt, further optimization work is needed to get better phase purity.

Step 2, in which the atmosphere is changed from Ar to O₂, is very important to form Yb123 from the melt. Our earlier

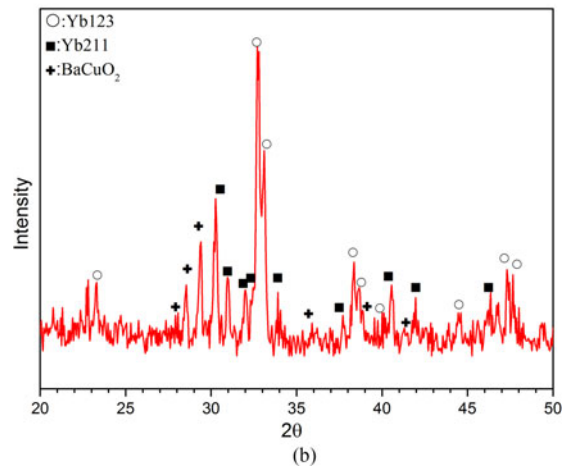
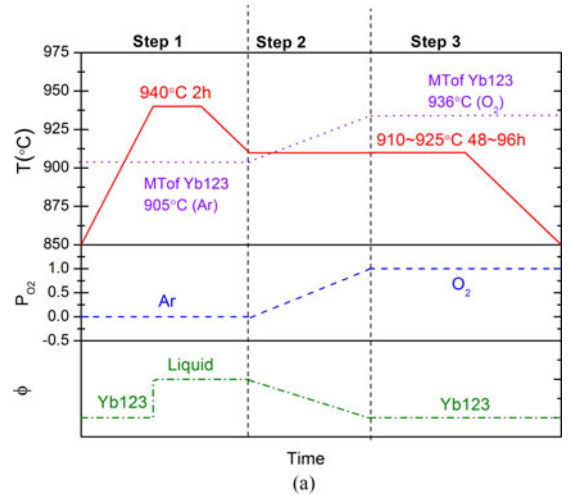


Fig. 1. (a) The heat treatment process designed for Yb123/Ag tape. The three y axes from top to bottom are temperature (red solid line), pO₂ (blue dashed line), and phases (green dash-dot line), and the melt temperature of Yb123 in the Ag tape is shown as the purple dotted line. The pO₂ and melting temperature do not change linearly with time as shown in step 2, but it is adequate to show them as linear to indicate they are changing during the heat treatment. (b) XRD result of Yb123/Ag tape after the heat treatment shown in (a). A flow rate of 0.5 SCFH was used in step 2, which changed the atmosphere from Ar to pure O₂ in about 15 min.

studies showed that the pO₂ has a significant effect on the melt temperature of Yb123. We studied whether the rate at which O₂ replaced Ar in the furnace tube affected the nucleation and growth of Yb123 from the melt. In step 1, Ar flows through the tube furnace. In step 2, the Ar flow is stopped and replaced by O₂ flowing at different rates. Initially the pO₂ increases exponentially with time and then asymptotically approaches pure O₂, as shown in Fig. 2(a) and (b). The melting temperature of Yb123 changes with pO₂, which means that the melting temperature of Yb123 in step 2 does not decrease linearly with time as O₂ replaces Ar in the furnace tube. This is represented schematically in Fig. 1(a) by the purple dotted line. This non-linearity of the Yb123 melt temperature with pO₂ means controlling the melt temperature as the pO₂ is changed in step 2 is a complicated process.

Fig. 2(c) shows the time needed to reach 20% O₂ (approximately equivalent to pO₂ in air, which is 200,000 ppm) and pure

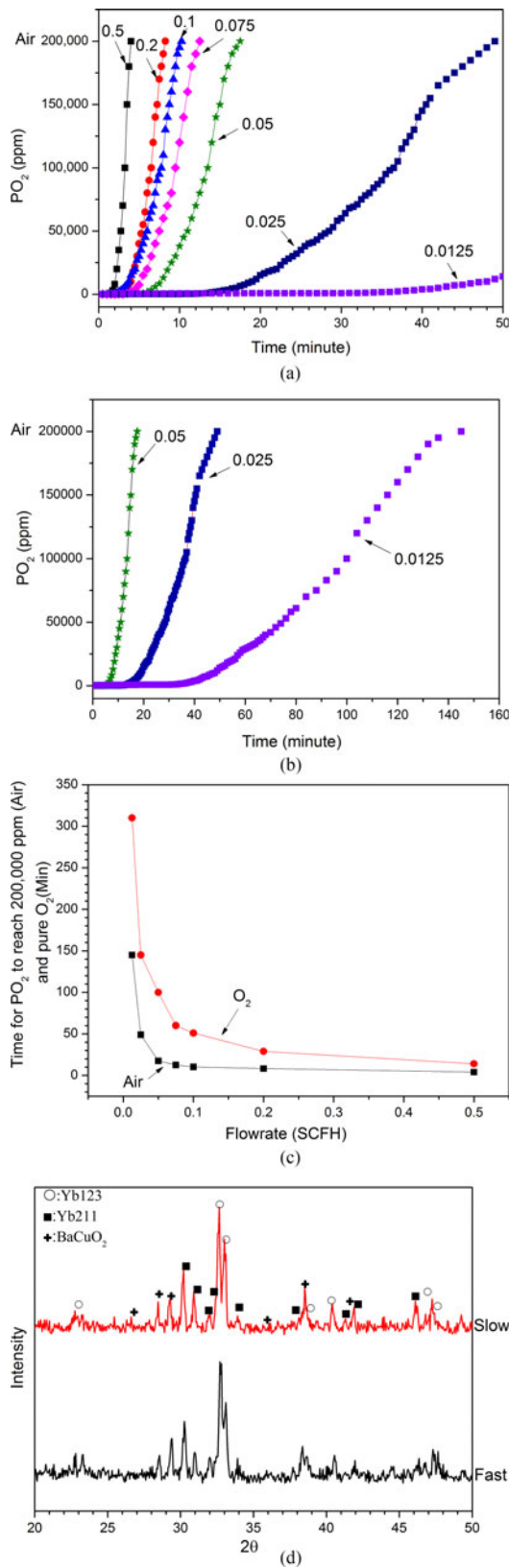


Fig. 2. (a) and (b) The pO_2 value in the tube furnace versus time with different flow rates. (c) The time for the pO_2 in the tube furnace to reach the pO_2 in air (200,000 ppm) and pure oxygen (1,000,000 ppm) with different flow rates. (d) The XRD results of fully heat-treated $\text{YbBa}_2\text{Cu}_3\text{O}_{7-\delta}$ /Ag tape different flow O_2 flow rates. Slow = 0.0125 SCFH and fast = 0.5 SCFH.

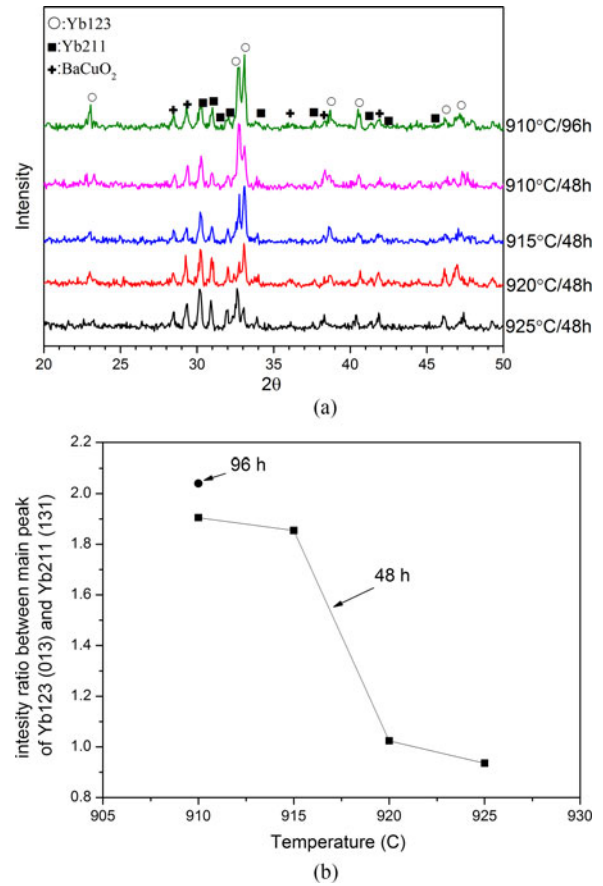


Fig. 3. (a) XRD results of fully heat-treated $\text{YbBa}_2\text{Cu}_3\text{O}_{7-\delta}$ /Ag tape for different temperatures and times. (b) The $\text{YbBa}_2\text{Cu}_3\text{O}_{7-\delta}$: $\text{YbBa}_2\text{Cu}_3\text{O}_{7-\delta}$ intensity ratio for different temperatures during step 3. All times shown are for 48 h, except for one heat treatment at 910 °C, which was for 96 h.

O_2 (1,000,000 ppm) in the furnace with different flow rates. It shows that the time to 20% O_2 is not significantly different using flow rates of 0.5 to 0.075 SCFH but the time to 20% O_2 is at least 10 times longer with a flow rate 0.0125 SCFH. We did experiments with a fast flow rate (0.5 SCFH) and a slow flow rate (0.0125 SCFH) to test what effect the rate at which the pO_2 was changed in step 2 has on the final phase purity. It shows the fast and slow flow rates need 14 and 340 min, respectively, to reach 1 atmosphere O_2 . Fig. 2(d) shows the XRD patterns of fully-processed $\text{YbBa}_2\text{Cu}_3\text{O}_{7-\delta}$ /Ag tape with these two flow rates are very similar, consisting of $\text{YbBa}_2\text{Cu}_3\text{O}_{7-\delta}$ as the main phase plus remnant $\text{YbBa}_2\text{Cu}_3\text{O}_{7-\delta}$ and BaCuO_2 impurity phases. The $\text{YbBa}_2\text{Cu}_3\text{O}_{7-\delta}$: $\text{YbBa}_2\text{Cu}_3\text{O}_{7-\delta}$ intensity ratio of samples with fast and slow flow rates are essentially the same (1.94 and 1.89, respectively). This result indicates that changing the O_2 flow rate is not the main factor determining the phase purity of the final product.

The temperature and time in step 3 is critical to reform $\text{YbBa}_2\text{Cu}_3\text{O}_{7-\delta}$. Various temperatures and times were investigated. Fig. 3(a) and (b) show the XRD patterns and the $\text{YbBa}_2\text{Cu}_3\text{O}_{7-\delta}$: $\text{YbBa}_2\text{Cu}_3\text{O}_{7-\delta}$ intensity ratio for different temperatures and times. All the samples have the same phases present, and in each case, $\text{YbBa}_2\text{Cu}_3\text{O}_{7-\delta}$ is the main phase. The strongest $\text{YbBa}_2\text{Cu}_3\text{O}_{7-\delta}$ peak alternated between (103) and (013) for different samples, which indicates random orientation

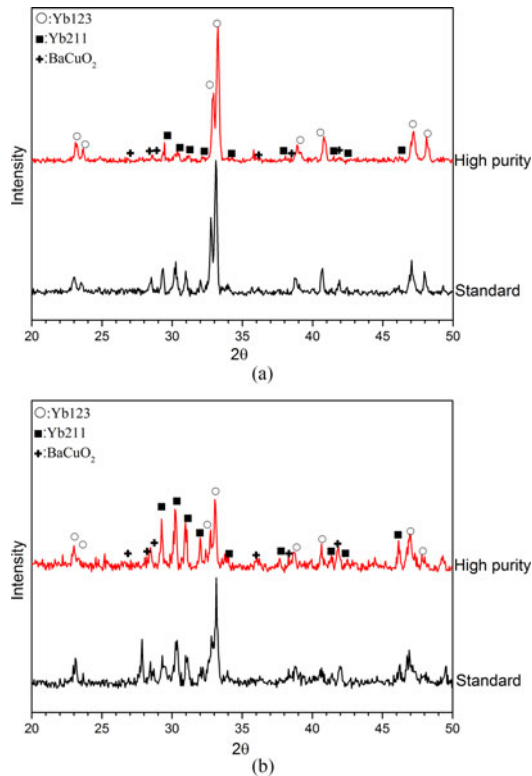


Fig. 4. XRD patterns from (a) as-synthesized Yb123 powders and (b) after the full heat treatment in Ag tape. The Yb123 powders had different purities. Standard purity indicates as-synthesized Yb123 powder with a Yb123:Yb211 intensity ratio of 4 and high purity has a ratio of 8.

of Yb123 after the regrowth process. Fig. 3(b) shows that slightly more Yb123 formed at 910 and 915 °C than at higher temperatures, but extending the time from 48 h to 96 h at 910 °C did not significantly increase the amount of Yb123 that formed. These results indicate that the heat treatment temperature and time are not the dominating factors in the formation of high purity Yb123.

We also investigated if the purity of as-synthesized Yb123 had a significant effect on the phase purity of the final product. We did this by comparing the Yb123 formation in tapes made with powder that had a Yb123:Yb211 ratio of 4 (standard purity) and 8 (high purity). Fig. 4(a) shows the x-ray pattern of the Yb123 powder with Yb123:Yb211 ratios of 4 and 8. Fig. 4(b) is the x-ray patterns after melting and regrowing Yb123 (step 3 has $T = 910^{\circ}\text{C}$ and $t = 48\text{ h}$), which shows that the tape made with the higher purity Yb123 powder formed a slightly smaller amount of Yb123 during regrowth. This seems counter intuitive and we do not have an explanation for this.

IV. CONCLUSION

A three-step heat treatment process had previously been established to melt and regrow Yb123 in a Yb123/Ag-sheathed

powder-in-tube tape. The Yb123 in the Ag tape can be successfully melted and reformed by manipulating the oxygen partial pressure and temperature. The Yb123 that reforms contains more impurity phases (Yb211 and BaCuO₂) than the as-synthesized Yb123 powder that was used to fabricate the tape. We investigated the effect that the rate at which the atmosphere was changed from flowing Ar to flowing O₂, and the heat treatment temperature and time in step 3 of the heat treatment have on the formation of Yb123. For the range of O₂ flow rates we used to change the atmosphere (from Ar to O₂), there was little effect on the formation of Yb123. The maximum amount of Yb123 formed for temperatures between 910 and 915 °C in step 3. Extending the time from 48 to 96 h at 910 °C did not form significantly more Yb123. When we melted and regrew Yb123 in a Yb123/Ag wire with purer Yb123 powder, the regrown Yb123 contained more impurities than when we started with less pure Yb123 powder. At present we do not have an explanation for this counter intuitive result.

REFERENCES

- [1] S. S. Fu *et al.*, "Electromagnetic characteristics analysis of core cable consisting of YBCO coated conductor," *IEEE Trans. Appl. Supercond.*, vol. 27, no. 4, Jun. 2017, Art. no. 4802805.
- [2] N. Bykovsky, D. Uglietti, K. Sedlak, B. Stepanov, R. Wesche, and P. Bruzzone, "Performance evolution of 60 kA HTS cable prototypes in the EDIPO test facility," *Supercond. Sci. Technol.*, vol. 29, no. 8, Aug. 2016, Art. no. 084002.
- [3] H. W. Weijers *et al.*, "Progress in the development and construction of a 32-T superconducting magnet," *IEEE Trans. Appl. Supercond.*, vol. 26, no. 4, Jun. 2016, Art. no. 4300807.
- [4] S. Awaji *et al.*, "First performance test of a 25 T cryogen-free superconducting magnet," *Supercond. Sci. Technol.*, vol. 30, no. 6, Jun. 2017, Art. no. 065001.
- [5] M. Majka, J. Kozak, and S. Kozak, "HTS tapes selection for superconducting current limiters," *IEEE Trans. Appl. Supercond.*, vol. 27, no. 4, Jun. 2017, Art. no. 5601405.
- [6] D. Y. Hu, Z. Y. Li, Z. Y. Hong, and Z. J. Jin, "Development of a single-phase 330 kVA HTS transformer using GdBCO tapes," *Physica C*, vol. 539, pp. 8–12, Aug. 2017.
- [7] J. S. Jeong, D. K. An, J. P. Hong, H. J. Kim, and Y. S. Jo, "Design of a 10-MW-class HTS homopolar generator for wind turbines," *IEEE Trans. Appl. Supercond.*, vol. 27, no. 4, Jun. 2017, Art. no. 5202804.
- [8] Y. Zhao, P. Torres, X. Tang, P. Norby, and J. C. Grivel, "Growth of highly epitaxial YBa₂Cu₃O_{7- δ} films from a simple propionates-based solution," *Inorg. Chem.*, vol. 54, no. 21, pp. 10232–10238, Oct. 2015.
- [9] Y. Zhao, W. Wu, X. Tang, N. H. Andersen, Z. Han, and J. C. Grivel, "Epitaxial growth of YBa₂Cu₃O_{7- x} films on Ce_{0.9}La_{0.1}O_{2- y} buffered yttria-stabilized zirconia substrates by an all-chemical-solution route," *Cryst. Eng. Comm.*, vol. 16, no. 21, pp. 4369–4372, Mar. 2014.
- [10] M. W. Rupich, X. Li, S. Sathyamurthy, C. Thieme, and S. Fleshler, "Advanced development of TFA-MOD coated conductors," *Physica C, Supercond. Appl.*, vol. 471, no. 21/22, pp. 919–923, Nov. 2011.
- [11] P. Paturi *et al.*, "Preparing superconducting nanopowder based YBCO/Ag tapes," *Physica C, Supercond.*, vol. 372–376, no. 2, pp. 779–781, Aug. 2002.
- [12] D. C. Larbalestier *et al.*, "Isotropic round-wire multifilament cuprate superconductor for generation of magnetic fields above 30 T," *Nat. Mater.*, vol. 13, no. 4, pp. 375–381, Apr. 2014.
- [13] M. Morita, S. Takebayashi, M. Tanaka, K. Kimura, K. Miyamoto, and K. Sawano, *Adv. Supercond. III*, Tokyo, Japan: Springer-Verlag, 1990, p. 733.